2026 IEEE/SICE International Symposium on System Integration (SII)
January 11-14, 2026. Cancún, México

Position and Attitude Estimation for Hydraulic Excavator Using External Sensors and Joint Angle Sensors

Kohki Yamamoto[1] and Ryo Kikuuwe[1]

Abstract— **This paper proposes an end-effector position and attitude estimation method for hydraulic excavators using total stations and potentiometers. The total station is an external sensor for measuring positions in a ground-fixed coordinate, but its sampling interval is too long for a position controller. The potentiometer is a joint angle sensor whose sampling interval suits the controller. The proposed method is an extended Kalman filter that simultaneously estimates position and attitude. It combines measurements from total stations and potentiometers with different sampling intervals to estimate accurate end-effector position and attitude with a short sampling interval. The proposed method's validity and applicability to the end-effector position control are verified using a real-time simulator of a hydraulic excavator.**

I. Introduction

Automation of hydraulic excavators is expected to improve the efficiency of tasks such as excavation and leveling of the ground. To achieve automation of hydraulic excavators, it is necessary to estimate and control the position and attitude of the end-effector accurately. One of commonly used external sensors at construction sites is the total station (TS). Although the TS can measure absolute position, its sampling time is too long to control excavators. Another sensor used to measure the joint angles of hydraulic excavators is the potentiometer (PM). The PMs are attached to each excavator's joint and measure joint angles, which allow for estimating the relative position of the end-effector from its body. In addition, PMs have a short sampling time, and thus they are suitable for controlling excavators.

Kalman filters have long been employed as a method for integrating multiple sensor values. Thalmann et al. [1] proposed a method that integrates measurements from TS and an inertial navigation system to estimate position and attitude. Since this method uses Euler angles, it may suffer from singularities. Many studies have used quaternions to represent position and attitude. Filipe et al. [2] proposed a method using dual quaternions for estimating the position and attitude of spacecraft. Dual quaternions can express position and attitude in a single structure, but there is an issue with complex implementation. Olofsson et al. [3] proposed a method for estimating the position and attitude of the end-effector of an industrial robot by combining its manipulator joint angles and IMU sensor values. This method treats position as a three-dimensional vector and attitude as a unit quaternion. A framework for integrating low-frequency sensor values, such as total station, and high-frequency sensor values, such as potentiometer, as used in this study, has not yet been sufficiently established.

This paper proposes an estimation method for the position and attitude of the end-effector of the excavator by integrating measurements from TS and PM. In the proposed method, position and attitude are treated as a single seven-dimensional vector, and an extended Kalman filter (EKF) is used to fuse the TS and PM measurements. The EKF depends on many Jacobian matrices involving the attitude quaternion, but their analytical, singularity-free expressions are presented in this paper. To address the difference in sampling intervals between TS and PM, the update step of the EKF is divided into two patterns, namely pattern A and pattern B. The pattern A updates the state using the PM values, and the pattern B updates the state using both the PM and TS values when the TS values are available. The validity of the proposed method and its applicability to end-effector position control were verified using a real-time simulator of a hydraulic excavator.

II. Position and Attitude in Coordinate Frames

A. Representation of Position and Attitude

One method for representing attitude is the use of quaternions. In this paper, $\mathbb{R}$ denotes the set of real numbers, and $\mathbb{H}$ denotes the set of unit quaternions. Since quaternions are treated as four-dimensional vectors, the relation $\mathbb{H} \subset \mathbb{R}^4$ holds. The attitude of a rigid body in three-dimensional space can be represented by the 3×3 rotation matrix of which the column vectors correspond to the axes of the body coordinate frame. The correspondence between a rotation matrix and a unit quaternion $\boldsymbol{a} = [a_w, a_x, a_y, a_z]^T \in \mathbb{H}$ is given by the following equation.

$$\mathrm{q2m}(\boldsymbol{a}) \triangleq \begin{bmatrix} a_w^2 + a_x^2 - a_y^2 - a_z^2 & 2(a_x a_y - a_w a_z) & 2(a_x a_z + a_w a_y) \\ 2(a_x a_y + a_w a_z) & a_w^2 - a_x^2 + a_y^2 - a_z^2 & 2(a_y a_z - a_w a_x) \\ 2(a_x a_z - a_w a_y) & 2(a_y a_z + a_w a_x) & a_w^2 - a_x^2 - a_y^2 + a_z^2 \end{bmatrix} \tag{1}$$

To handle the position and attitude of a rigid body in a compact form, the set $\mathbb{P} \triangleq \mathbb{R}^3 \times \mathbb{H} \subset \mathbb{R}^7$ is used. Accordingly, the position $\boldsymbol{r} \in \mathbb{R}^3$ and the attitude $\boldsymbol{a} \in \mathbb{H}$ of the rigid body are represented as $\boldsymbol{p} \triangleq [\boldsymbol{r}^T, \boldsymbol{a}^T]^T \in \mathbb{P}$. The time derivative of $\boldsymbol{p} = [\boldsymbol{r}^T, \boldsymbol{a}^T]^T$ is given by $\boldsymbol{v} \triangleq [\dot{\boldsymbol{r}}^T, \mathring{\boldsymbol{a}}^T]^T \in \mathbb{R}^6$ where the operator $\circ$ is defined in Appendix. In addition, the addition operator $\oplus$, the subtraction operator $\ominus$, the multiplication operator $\otimes$, and the time derivative operator $\circ$ are used, of

[1]Machinery Dynamics Laboratory, Hiroshima University, 1-4-1 Kagamiyama, Higashi-Hiroshima, Hiroshima 739-8527, Japan. (e-mail: k.yamamoto@mdl.hiroshima-u.ac.jp; kikuuwe@ieee.org)

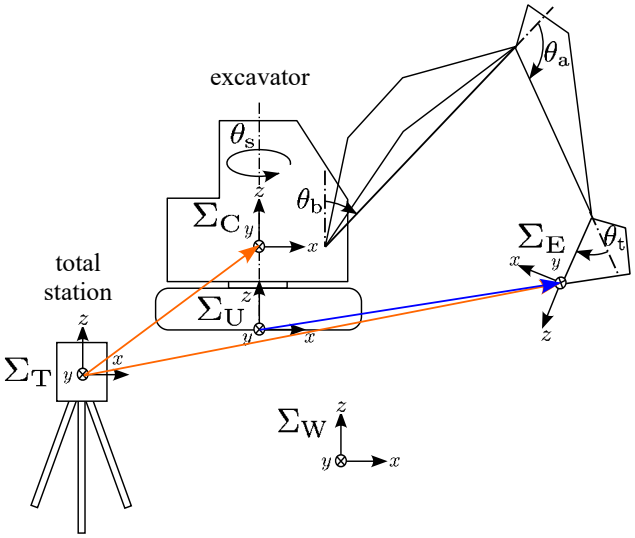

Fig. 1. Coordinate frames.

which the definitions and detailed computational procedures are given in Appendix.

B. Coordinate Frames

As shown in Fig. 1, this paper employs five coordinate frames, which are a world coordinate frame, a TS coordinate frame, an undercarriage frame, a cab coordinate frame, and an end-effector coordinate frame. The world coordinate frame, denoted by Σ_{W}, is fixed to the ground. The TS coordinate frame, denoted by Σ_{T}, is fixed to the TS. The undercarriage coordinate frame, denoted by Σ_{U}, is fixed to the excavator's undercarriage. The cab coordinate frame, denoted by Σ_{C}, is fixed to the body of the excavator. The end-effector coordinate frame, denoted by Σ_{E}, is fixed to the end-effector.

C. Coordinate Transformation of Position and Attitude

The end-effector position and attitude of the excavator can be expressed as ${}^{\mathrm{U}}\boldsymbol{p}_{\mathrm{EU}} = \boldsymbol{\Phi}(\boldsymbol{\theta})$, where $\boldsymbol{\theta} = [\theta_{\mathrm{s}}, \theta_{\mathrm{b}}, \theta_{\mathrm{a}}, \theta_{\mathrm{t}}]^T$ denotes the joint angles measured by the PM, and $\boldsymbol{\Phi}$ represents the forward kinematics. Here, ${}^{\mathrm{U}}\boldsymbol{p}_{\mathrm{EU}}$ denotes the position and attitude of the end-effector coordinate frame relative to the undercarriage coordinate frame, expressed in the undercarriage coordinate frame.

The TS can measure the position and attitude ${}^{\mathrm{T}}\boldsymbol{p}_{\mathrm{CT}}$ of the cab coordinate frame in the TS coordinate frame, and the position and attitude ${}^{\mathrm{T}}\boldsymbol{p}_{\mathrm{ET}}$ of the end-effector coordinate frame in the TS coordinate frame. Specifically, the TSs measure the positions of three targets attached to the cab and three targets attached to the end-effector. The position and attitude of each body are then calculated from the relative positions of its three targets. In practical excavation situations, the end-effector may not be visible to the TS because it can be embedded in the soil. In this study, ideal TS observations are assumed for the evaluation of the proposed estimator. The PM can measure the position and attitude ${}^{\mathrm{U}}\boldsymbol{p}_{\mathrm{EU}}$ of the end-effector coordinate frame, and the position and attitude ${}^{\mathrm{C}}\boldsymbol{p}_{\mathrm{UC}}$ of the undercarriage coordinate frame in the cab coordinate frame. From this, the position and attitude of the end-effector coordinate frame in the world coordinate frame can be expressed as follows:

$$ {}^{\mathrm{W}}\boldsymbol{p}_{\mathrm{EW}} = {}^{\mathrm{W}}\boldsymbol{p}_{\mathrm{TW}} \otimes {}^{\mathrm{T}}\boldsymbol{p}_{\mathrm{ET}} \tag{2} $$

$$ {}^{\mathrm{W}}\boldsymbol{p}_{\mathrm{EW}} = (({}^{\mathrm{W}}\boldsymbol{p}_{\mathrm{TW}} \otimes {}^{\mathrm{T}}\boldsymbol{p}_{\mathrm{CT}}) \otimes {}^{\mathrm{C}}\boldsymbol{p}_{\mathrm{UC}}) \otimes {}^{\mathrm{U}}\boldsymbol{p}_{\mathrm{EU}} \tag{3} $$

where ${}^{\mathrm{W}}\boldsymbol{p}_{\mathrm{TW}}$ is a constant, which is represented the position and attitude of the TS coordinate frame in the world coordinate frame.

The position and attitude ${}^{\mathrm{W}}\boldsymbol{p}_{\mathrm{UW}}$ of the undercarriage coordinate frame in the world coordinate frame is a reference value for estimating and controlling the position and attitude of excavator, and it can be described as follows:

$$ {}^{\mathrm{W}}\boldsymbol{p}_{\mathrm{UW}} = ({}^{\mathrm{W}}\boldsymbol{p}_{\mathrm{TW}} \otimes {}^{\mathrm{T}}\boldsymbol{p}_{\mathrm{CT}}) \otimes {}^{\mathrm{C}}\boldsymbol{p}_{\mathrm{UC}} \tag{4} $$

III. Position and Attitude Estimator and Position Controller

A. Extended Kalman Filter (EKF)

This section presents an Extended Kalman filter (EKF) to estimate the position and attitude of the end-effector. It is built on the state-space representation of a second-order integrator of positions and attitudes, which is as follows:

$$ \boldsymbol{x}(k+1) = \boldsymbol{f}(\boldsymbol{x}(k)) \oplus \boldsymbol{w} \tag{5} $$

$$ \begin{cases} \boldsymbol{y}_{\mathrm{A}}(k) = \boldsymbol{h}_{\mathrm{A}}(\boldsymbol{x}(k)) \oplus \boldsymbol{e}_{\mathrm{A}} \\ \boldsymbol{y}_{\mathrm{B}}(k) = \boldsymbol{h}_{\mathrm{B}}(\boldsymbol{x}(k)) \oplus \boldsymbol{e}_{\mathrm{B}} \end{cases} \tag{6} $$

where the state vector $\boldsymbol{x} \in \mathbb{R}^{32}$ is given as follows:

$$ \boldsymbol{x} = \left[{}^{\mathrm{W}}\boldsymbol{p}_{\mathrm{UW}}{}^T,\ {}^{\mathrm{W}}\boldsymbol{v}_{\mathrm{UW}}{}^T,\ {}^{\mathrm{U}}\boldsymbol{p}_{\mathrm{EU}}{}^T,\ {}^{\mathrm{U}}\boldsymbol{v}_{\mathrm{EU}}{}^T,\ {}^{\mathrm{U}}\dot{\boldsymbol{v}}_{\mathrm{EU}}{}^T \right]^T \tag{7} $$

Here, ${}^{\mathrm{W}}\boldsymbol{p}_{\mathrm{UW}}$ denotes the position and attitude of the undercarriage and ${}^{\mathrm{W}}\boldsymbol{v}_{\mathrm{UW}}$ denotes its linear velocity and angular velocity. ${}^{\mathrm{U}}\boldsymbol{p}_{\mathrm{EU}}$ denotes the position and attitude of the end-effector, ${}^{\mathrm{U}}\boldsymbol{v}_{\mathrm{EU}}$ denotes its linear and angular velocity, and ${}^{\mathrm{U}}\dot{\boldsymbol{v}}_{\mathrm{EU}}$ denotes its linear and angular acceleration. The state-space representation treats the process noise $\boldsymbol{w} \in \mathbb{R}^{30}$, the measurement noise $\boldsymbol{e}_{\mathrm{A}} \in \mathbb{R}^{6}$ and $\boldsymbol{e}_{\mathrm{B}} \in \mathbb{R}^{12}$, and the measurement vectors $\boldsymbol{y}_{\mathrm{A}} \in \mathbb{R}^{7}$ and $\boldsymbol{y}_{\mathrm{B}} \in \mathbb{R}^{14}$. Here, the subscripts A and B are used to distinguish the two types of measurement vectors. Specifically, the subscript A denotes the measurement vector consisting of PM values, while the subscript B denotes the measurement vector consisting of both PM and TS values. The nonlinear functions are given by $\boldsymbol{f} : \mathbb{R}^{32} \to \mathbb{R}^{32}$, $\boldsymbol{h}_{\mathrm{A}} : \mathbb{R}^{7} \to \mathbb{R}^{7}$, and $\boldsymbol{h}_{\mathrm{B}} : \mathbb{R}^{14} \to \mathbb{R}^{14}$. The nonlinear functions $\boldsymbol{f}$, $\boldsymbol{h}_{\mathrm{A}}$, and $\boldsymbol{h}_{\mathrm{B}}$ defined as follows.

$$ \boldsymbol{f}(\boldsymbol{x}(k)) = \begin{bmatrix} {}^{\mathrm{W}}\boldsymbol{p}_{\mathrm{UW}} \oplus T\,{}^{\mathrm{W}}\boldsymbol{v}_{\mathrm{UW}} \\ {}^{\mathrm{W}}\boldsymbol{v}_{\mathrm{UW}} \\ {}^{\mathrm{U}}\boldsymbol{p}_{\mathrm{EU}} \oplus T({}^{\mathrm{U}}\boldsymbol{v}_{\mathrm{EU}} + \frac{T}{2}\,{}^{\mathrm{U}}\dot{\boldsymbol{v}}_{\mathrm{EU}}) \\ {}^{\mathrm{U}}\boldsymbol{v}_{\mathrm{EU}} + T\,{}^{\mathrm{U}}\dot{\boldsymbol{v}}_{\mathrm{EU}} \\ {}^{\mathrm{U}}\dot{\boldsymbol{v}}_{\mathrm{EU}} \end{bmatrix} \tag{8} $$

$$ \boldsymbol{h}_{\mathrm{A}}(\boldsymbol{x}(k)) = {}^{\mathrm{U}}\boldsymbol{p}_{\mathrm{EU}} \tag{9} $$

$$ \boldsymbol{h}_{\mathrm{B}}(\boldsymbol{x}(k)) = \begin{bmatrix} {}^{\mathrm{U}}\boldsymbol{p}_{\mathrm{EU}} \\ {}^{\mathrm{W}}\boldsymbol{p}_{\mathrm{UW}} \otimes {}^{\mathrm{U}}\boldsymbol{p}_{\mathrm{EU}} \end{bmatrix} \tag{10} $$

These nonlinear functions $\boldsymbol{f}$, $\boldsymbol{h}_{\mathrm{A}}$, and $\boldsymbol{h}_{\mathrm{B}}$ are linearized around the current estimates as follows:

$$\boldsymbol{F} = \left(\frac{\mathring{\partial} \boldsymbol{f}}{\mathring{\partial} \boldsymbol{x}} \right)_{\boldsymbol{x}=\hat{\boldsymbol{x}}(k|k)} = \begin{bmatrix} \frac{\mathring{\partial} \boldsymbol{f}}{\mathring{\partial}\, {}^{\mathrm{W}}\boldsymbol{p}_{\mathrm{UW}}} & \frac{\mathring{\partial} \boldsymbol{f}}{\partial\, {}^{\mathrm{W}}\boldsymbol{v}_{\mathrm{UW}}} & \boldsymbol{0} & \boldsymbol{0} & \boldsymbol{0} \\ \boldsymbol{0} & \boldsymbol{I}_6 & \boldsymbol{0} & \boldsymbol{0} & \boldsymbol{0} \\ \boldsymbol{0} & \boldsymbol{0} & \frac{\mathring{\partial} \boldsymbol{f}}{\mathring{\partial}\, {}^{\mathrm{U}}\boldsymbol{p}_{\mathrm{EU}}} & \frac{\mathring{\partial} \boldsymbol{f}}{\partial\, {}^{\mathrm{U}}\boldsymbol{v}_{\mathrm{EU}}} & \frac{\mathring{\partial} \boldsymbol{f}}{\partial\, {}^{\mathrm{U}}\dot{\boldsymbol{v}}_{\mathrm{EU}}} \\ \boldsymbol{0} & \boldsymbol{0} & \boldsymbol{0} & \boldsymbol{I}_6 & T\boldsymbol{I}_6 \\ \boldsymbol{0} & \boldsymbol{0} & \boldsymbol{0} & \boldsymbol{0} & \boldsymbol{I}_6 \end{bmatrix}_{\boldsymbol{x}=\hat{\boldsymbol{x}}(k|k)} \tag{11a}$$

$$\boldsymbol{H}_{\mathrm{A}} = \left(\frac{\mathring{\partial} \boldsymbol{h}_{\mathrm{A}}}{\mathring{\partial} \boldsymbol{x}} \right)_{\boldsymbol{x}=\hat{\boldsymbol{x}}(k|k-1)} = \begin{bmatrix} \boldsymbol{0} & \boldsymbol{0} & \boldsymbol{I}_6 & \boldsymbol{0} & \boldsymbol{0} \end{bmatrix}_{\boldsymbol{x}=\hat{\boldsymbol{x}}(k|k-1)} \tag{11b}$$

$$\boldsymbol{H}_{\mathrm{B}} = \left(\frac{\mathring{\partial} \boldsymbol{h}_{\mathrm{B}}}{\mathring{\partial} \boldsymbol{x}} \right)_{\boldsymbol{x}=\hat{\boldsymbol{x}}(k|k-1)} = \begin{bmatrix} \boldsymbol{0} & \boldsymbol{0} & \boldsymbol{I}_6 & \boldsymbol{0} & \boldsymbol{0} \\ \frac{\mathring{\partial} \boldsymbol{h}_{\mathrm{B}}}{\mathring{\partial}\, {}^{\mathrm{W}}\boldsymbol{p}_{\mathrm{UW}}} & \boldsymbol{0} & \frac{\mathring{\partial} \boldsymbol{h}_{\mathrm{B}}}{\mathring{\partial}\, {}^{\mathrm{U}}\boldsymbol{p}_{\mathrm{EU}}} & \boldsymbol{0} & \boldsymbol{0} \end{bmatrix}_{\boldsymbol{x}=\hat{\boldsymbol{x}}(k|k-1)} \tag{11c}$$

By using them, the algorithm of the proposed estimator is given as follows:

$$\hat{\boldsymbol{x}}(k|k-1) := \boldsymbol{f}(\hat{\boldsymbol{x}}(k-1|k-1)) \tag{12a}$$

$$\hat{\boldsymbol{P}}(k|k-1) := \boldsymbol{F}\hat{\boldsymbol{P}}(k-1|k-1)\boldsymbol{F}^T + \boldsymbol{Q} \tag{12b}$$

if only PM values are available then

$$\boldsymbol{K}_{\mathrm{A}} := \hat{\boldsymbol{P}}(k|k-1)\boldsymbol{H}_{\mathrm{A}}(\boldsymbol{H}_{\mathrm{A}}\hat{\boldsymbol{P}}(k|k-1)\boldsymbol{H}_{\mathrm{A}}{}^T + \boldsymbol{R}_{\mathrm{A}})^{-1} \tag{12c}$$

$$\hat{\boldsymbol{x}}(k|k) := \hat{\boldsymbol{x}}(k|k-1) \oplus \boldsymbol{K}_{\mathrm{A}}(\boldsymbol{y}_{\mathrm{A}}(k) \ominus \boldsymbol{h}_{\mathrm{A}}(\hat{\boldsymbol{x}}(k|k-1))) \tag{12d}$$

$$\hat{\boldsymbol{P}}(k|k) := (\boldsymbol{I} - \boldsymbol{K}_{\mathrm{A}}\boldsymbol{H}_{\mathrm{A}})\hat{\boldsymbol{P}}(k|k-1) \tag{12e}$$

else if both PM and TS values are available then

$$\boldsymbol{K}_{\mathrm{B}} := \hat{\boldsymbol{P}}(k|k-1)\boldsymbol{H}_{\mathrm{B}}(\boldsymbol{H}_{\mathrm{B}}\hat{\boldsymbol{P}}(k|k-1)\boldsymbol{H}_{\mathrm{B}}{}^T + \boldsymbol{R}_{\mathrm{B}})^{-1} \tag{12f}$$

$$\hat{\boldsymbol{x}}(k|k) := \hat{\boldsymbol{x}}(k|k-1) \oplus \boldsymbol{K}_{\mathrm{B}}(\boldsymbol{y}_{\mathrm{B}}(k) \ominus \boldsymbol{h}_{\mathrm{B}}(\hat{\boldsymbol{x}}(k|k-1))) \tag{12g}$$

$$\hat{\boldsymbol{P}}(k|k) := (\boldsymbol{I} - \boldsymbol{K}_{\mathrm{B}}\boldsymbol{H}_{\mathrm{B}})\hat{\boldsymbol{P}}(k|k-1) \tag{12h}$$

end if

where the matrix $\boldsymbol{P} \in \mathbb{R}^{30\times30}$ denotes the error covariance matrix, and the matrix $\boldsymbol{Q} \in \mathbb{R}^{30\times30}$ denotes the process noise covariance matrix. The Kalman gain are given by $\boldsymbol{K}_{\mathrm{A}} \in \mathbb{R}^{6\times30}$ and $\boldsymbol{K}_{\mathrm{B}} \in \mathbb{R}^{12\times30}$, and the observation noise covariance matrices are denoted by $\boldsymbol{R}_{\mathrm{A}} \in \mathbb{R}^{6\times6}$ and $\boldsymbol{R}_{\mathrm{B}} \in \mathbb{R}^{12\times12}$. The covariance matrices $\boldsymbol{Q}$, $\boldsymbol{R}_{\mathrm{A}}$, and $\boldsymbol{R}_{\mathrm{B}}$ are defined as follows:

$$\boldsymbol{Q} = \mathrm{block\,diag}(10^{-5}\boldsymbol{I}_6, 10^{-2}\boldsymbol{I}_6, 10^{-7}\boldsymbol{I}_6, 10^{-5}\boldsymbol{I}_6, 10^{-2}\boldsymbol{I}_6) \tag{13a}$$

$$\boldsymbol{R}_{\mathrm{A}} = \mathrm{block\,diag}(10^{-5}\boldsymbol{I}_6) \tag{13b}$$

$$\boldsymbol{R}_{\mathrm{B}} = \mathrm{block\,diag}(10^{-5}\boldsymbol{I}_6, 10^{-19}\boldsymbol{I}_6) \tag{13c}$$

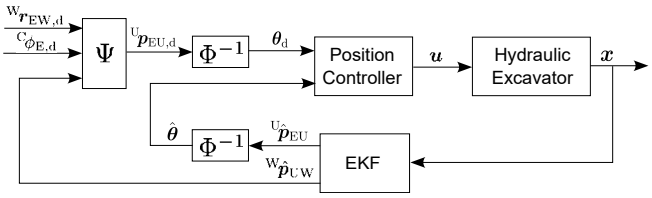

Fig. 2. Overview of the control system.

B. Generation of Joint Angle References

An overview of the end-effector position control is shown in Fig. 2. The target position of the end-effector is denoted by ${}^{\mathrm{W}}\boldsymbol{r}_{\mathrm{EW,d}} \in \mathbb{R}^3$, and the target attitude of the end-effector is denoted by ${}^{\mathrm{C}}\phi_{\mathrm{E,d}} \in \mathbb{R}$. Here, ${}^{\mathrm{C}}\phi_{\mathrm{E,d}}$ represents the target tilt angle of the end-effector coordinate frame seen from the cab coordinate frame, and is given by ${}^{\mathrm{C}}\phi_{\mathrm{E,d}} = \theta_{\mathrm{b,d}} + \theta_{\mathrm{a,d}} + \theta_{\mathrm{t,d}}$. The variables $\theta_{\mathrm{b,d}}$, $\theta_{\mathrm{a,d}}$, and $\theta_{\mathrm{t,d}}$ denote the desired values of the joint angles θ_{b}, θ_{a}, and θ_{t}, respectively. The target position ${}^{\mathrm{W}}\boldsymbol{r}_{\mathrm{EW,d}} \in \mathbb{R}^3$, the target attitude ${}^{\mathrm{C}}\phi_{\mathrm{E,d}}$, and the estimated undercarriage position and attitude ${}^{\mathrm{W}}\hat{\boldsymbol{p}}_{\mathrm{UW}}$ are used to express the target end-effector position and attitude seen from the undercarriage coordinate frame. The target position and attitude ${}^{\mathrm{U}}\boldsymbol{p}_{\mathrm{EU,d}}$ is expressed using a function Ψ as follows:

$${}^{\mathrm{U}}\boldsymbol{p}_{\mathrm{EU,d}} = \Psi({}^{\mathrm{W}}\boldsymbol{r}_{\mathrm{EW,d}}, {}^{\mathrm{C}}\phi_{\mathrm{E,d}}, {}^{\mathrm{W}}\hat{\boldsymbol{p}}_{\mathrm{UW}}) \tag{14}$$

The estimated end-effector position and attitude ${}^{\mathrm{U}}\hat{\boldsymbol{p}}_{\mathrm{EU}}$ and the target end-effector position and attitude ${}^{\mathrm{U}}\boldsymbol{p}_{\mathrm{EU,d}}$ are converted to the estimated joint angles $\hat{\boldsymbol{\theta}} = [\hat{\theta}_{\mathrm{s}}, \hat{\theta}_{\mathrm{b}}, \hat{\theta}_{\mathrm{a}}, \hat{\theta}_{\mathrm{t}}]^T$ and the target joint angles $\boldsymbol{\theta}_{\mathrm{d}} = [\theta_{\mathrm{s,d}}, \theta_{\mathrm{b,d}}, \theta_{\mathrm{a,d}}, \theta_{\mathrm{t,d}}]^T$ by using the inverse kinematics Φ^{-1}, respectively. These relationships are written as follows:

$$\boldsymbol{\theta}_{\mathrm{d}}(k) = \boldsymbol{\Phi}^{-1}({}^{\mathrm{U}}\boldsymbol{p}_{\mathrm{EU,d}}(k)) \tag{15}$$

$$\hat{\boldsymbol{\theta}}(k) = \boldsymbol{\Phi}^{-1}({}^{\mathrm{U}}\hat{\boldsymbol{p}}_{\mathrm{EU}}(k)) \tag{16}$$

Here, the inverse kinematics $\boldsymbol{\Phi}^{-1}$ is assumed that each joint of the excavator bends only in a single specified direction. This paper employs a position controller for hydraulic excavators [4]. Its input is these joint angles $\boldsymbol{\theta}_{\mathrm{d}}$ and $\hat{\boldsymbol{\theta}}$, and its output is valve opening ratios $\boldsymbol{u}$ of hydraulic actuators.

IV. Simulations

A. Setup

Simulations were conducted using a real-time simulator [5] of a hydraulic excavator. It is based on a quasi-static model [6] of hydraulic actuators. Fig. 3(a) shows two devices and the simulator's screen. The end-effector of the excavator can be moved by operating these devices. Fig. 3(b) shows the excavator in the simulator. The undercarriage of the excavator is fixed to the ground. The ground surface is inclined by 0.2 rad from a horizontal plane. The proposed estimator and controller were implemented in MATLAB/Simulink with a sampling interval $T = 1.0 \times 10^{-2}$ s. In the simulator, each actuator and link of the excavator is virtually connected by

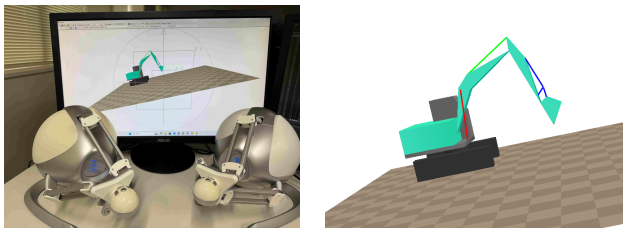

(a) Devices and simulator's screen. (b) Excavator on a slope.

Fig. 3. Simulation environment.

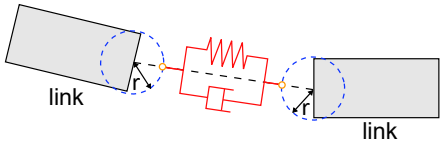

Fig. 4. Joint.

spring-damper elements, and each joint has a clearance with a radius of $r = 1.0 \times 10^{-3}$ m as shown in Fig. 4.

The TS and PM values are sent to MATLAB/Simulink with sampling intervals $T_{\mathrm{TS}} = 0.3$ s and $T_{\mathrm{PM}} = 1.0 \times 10^{-2}$ s, respectively. Low-pass filtered white noise signals were added to the PM values [7], and their cutoff frequency and standard deviation were set as 100 Hz and 5.0×10^{-4} rad, respectively. The TS values were obtained from the true end-effector and cab positions and attitudes at the TS sampling interval, assuming ideal observations.

B. Scenario 1: Excavator on a Slope

In Scenario 1, the end-effector position vector and attitude quaternion were estimated while the end-effector of the excavator was manually operated using two devices. The estimation results are shown in Fig. 5. Fig. 5(a) shows the actual end-effector position vector and the error between the estimated values and the actual values. Fig. 5(b) shows the actual end-effector attitude quaternion and the error between the estimated values and the actual values. Fig. 5(c) shows the snapshots of this simulation. The excavator remained stationary during $t \in [0\ \mathrm{s}, 5\ \mathrm{s}]$ and $t \in [28\ \mathrm{s}, 30\ \mathrm{s}]$. It performed a swinging motion during $t \in [5\ \mathrm{s}, 12\ \mathrm{s}]$, and a digging motion during $t \in [12\ \mathrm{s}, 28\ \mathrm{s}]$. The estimation error for each component of the position vector was less than 0.03 m, and the error for each component of the attitude quaternion was less than 5.0×10^{-3}.

C. Scenario 2: Position Control of Excavator on a Slope

In Scenario 2, the end-effector position vector and attitude quaternion were estimated while the end-effector of the excavator was position-controlled. The estimation results are shown in Fig. 6. Fig. 6(a) shows the actual end-effector position vector and the error between the estimated values and the actual values. Fig. 6(b) shows the actual end-effector attitude quaternion and the error between the estimated values and the actual values. Fig. 6(c) shows the snapshots of this simulation. The excavator remained stationary during $t \in [0\ \mathrm{s}, 10\ \mathrm{s}]$. Subsequently, its end-effector was moved

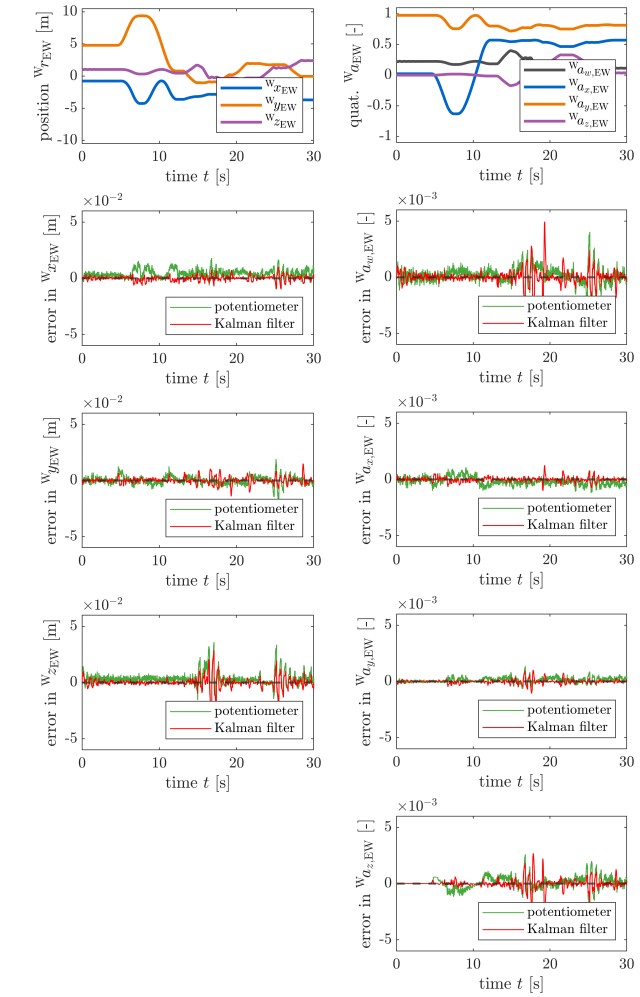

(a) End-effector position vector. (b) End-effector quaternion.

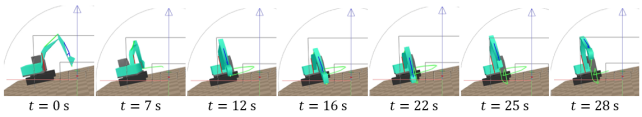

(c) Snapshots of a simulation.

Fig. 5. Estimation results of Scenario 1.

along a straight trajectory toward the position ${}^{\mathrm{W}}\boldsymbol{r}_{\mathrm{EW,d}} = [0.5\ \mathrm{m}, 1.0\ \mathrm{m}, 0.25\ \mathrm{m}]$ and attitude ${}^{\mathrm{C}}\phi_{\mathrm{E,d}} = \pi$ rad. The estimation error for each component of the position vector was less than 0.01 m, and the error for each component of the attitude quaternion was less than 2.0×10^{-3}.

The position control result is shown in Fig. 7. The black sphere shows the target position, and the red line shows the end-effector trajectory.

D. Discussion of Simulation Results

Based on the results of Scenarios 1 and 2, the proposed method enables the proper estimation of the end-effector position vector and attitude quaternion. The estimated values resulted in smaller offsets than PM values, however there were instances where the errors between estimates and true values exceeded those of PM values. This behavior may be attributed to an insufficient tuning of the process

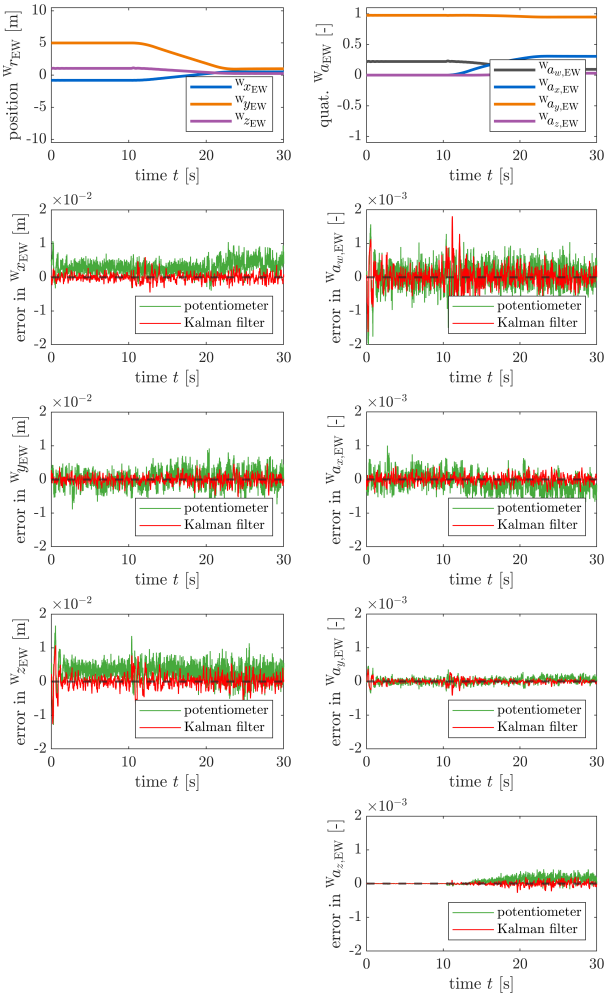

(a) End-effector position vector. (b) End-effector quaternion.

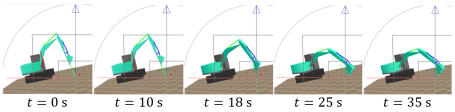

(c) Snapshots of a simulation.

Fig. 6. Estimation results of Scenario 2.

noise covariance matrix. In addition, the results of the end-effector position control show that the end-effector position converged to the target position. These results validate and apply the proposed position and attitude estimation method to end-effector position control.

V. Conclusion

This paper has proposed the estimation method for the end-effector of the hydraulic excavator using TS and PM values. The proposed method estimates the end-effector position and attitude simultaneously. The EKF's update step was divided into two patterns to address the difference in sampling intervals between TS and PM. The pattern A updates the state using the PM values, and the pattern B updates the state using both the PM and TS values. The proposed estimator was validated using the real-time simulator.

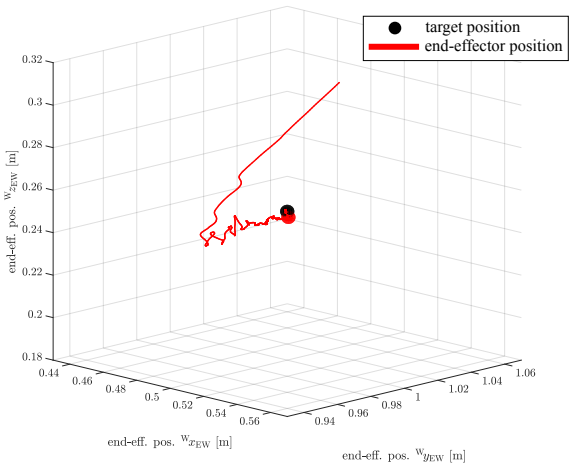

Fig. 7. Control result of Scenario 2.

Future work should focus on improving the simulation environment. In the real world, the total station may fail to measure target points when occluded by soil or surrounding structures. To evaluate the robustness of the proposed method under such conditions, these occlusion cases should be incorporated into the simulation to reflect practical environments.

Appendix

The time derivative operator $\circ$ of a quaternion is defined as follows:

$$\mathring{\boldsymbol{a}} \triangleq 2 \begin{bmatrix} -a_x & a_w & -a_z & a_y \\ -a_y & a_z & a_w & -a_x \\ -a_z & -a_y & a_x & a_w \end{bmatrix} \begin{bmatrix} \dot{a}_w \\ \dot{a}_x \\ \dot{a}_y \\ \dot{a}_z \end{bmatrix} \tag{17}$$

With this operator, the angular velocity $\boldsymbol{\omega} \in \mathbb{R}^3$ and the attitude $\boldsymbol{a} \in \mathbb{H}$ of a rigid body can be associated as $\boldsymbol{\omega} = \mathring{\boldsymbol{a}}$.

The quaternion multiplication $\otimes : \mathbb{H} \times \mathbb{H} \to \mathbb{H}$ is defined as follows:

$$\begin{bmatrix} a_w \\ a_x \\ a_y \\ a_z \end{bmatrix} \otimes \begin{bmatrix} b_w \\ b_x \\ b_y \\ b_z \end{bmatrix} \triangleq \begin{bmatrix} a_w b_w - a_x b_x - a_y b_y - a_z b_z \\ a_x b_w + a_w b_x - a_z b_y + a_y b_z \\ a_y b_w + a_z b_x + a_w b_y - a_x b_z \\ a_z b_w - a_y b_x + a_x b_y + a_w b_z \end{bmatrix} \tag{18}$$

Based on this, the operators $\ominus : \mathbb{H} \times \mathbb{H} \to \mathbb{R}^3$ and $\oplus : \mathbb{H} \times \mathbb{R}^3 \to \mathbb{H}$ are defined as follows:

$$\boldsymbol{a} \ominus \boldsymbol{b} \triangleq \mathrm{q2v}\left(\boldsymbol{a} \otimes \mathrm{inv}(\boldsymbol{b})\right) \tag{19}$$

$$\boldsymbol{a} \oplus \boldsymbol{r} \triangleq \mathrm{v2q}(\boldsymbol{r}) \otimes \boldsymbol{a} \tag{20}$$

Here, $\mathrm{inv} : \mathbb{H} \to \mathbb{H}$, $\mathrm{q2v} : \mathbb{H} \to \mathbb{R}^3$ and $\mathrm{v2q} : \mathbb{R}^3 \to \mathbb{H}$ are defined as follows:

$$\mathrm{inv}\left(\begin{bmatrix} a_w \\ \boldsymbol{a}_{xyz} \end{bmatrix}\right) \triangleq \begin{bmatrix} a_w \\ -\boldsymbol{a}_{xyz} \end{bmatrix} \tag{21}$$

$$\mathrm{q2v}\left(\begin{bmatrix} a_w \\ \boldsymbol{a}_{xyz} \end{bmatrix}\right) \triangleq \frac{2\,\mathrm{sgn}(a_w)}{\mathrm{sinc}\left(\mathrm{asin}(\|\boldsymbol{a}_{xyz}\|)\right)} \boldsymbol{a}_{xyz} \tag{22}$$

$$\mathrm{v2q}\left(\boldsymbol{r}\right) \triangleq \begin{bmatrix} \cos(\|\boldsymbol{r}\|/2) \\ \boldsymbol{r}\,\mathrm{sinc}(\|\boldsymbol{r}\|/2)/2 \end{bmatrix} \tag{23}$$

where $\mathrm{sinc}(x) \triangleq \sin(x)/x$.

This paper uses the operators $\ominus$ and $\oplus$ also for the set $\mathbb{P} \triangleq \mathbb{R}^3 \times \mathbb{H}$, not only for the set $\mathbb{H}$. Specifically, the operators $\ominus : \mathbb{P} \times \mathbb{P} \to \mathbb{R}^6$, $\oplus : \mathbb{P} \times \mathbb{R}^6 \to \mathbb{P}$, and $\otimes : \mathbb{P} \times \mathbb{P} \to \mathbb{P}$ are defined as follows:

$$\begin{bmatrix} \boldsymbol{r}_1 \\ \boldsymbol{a}_1 \end{bmatrix} \ominus \begin{bmatrix} \boldsymbol{r}_2 \\ \boldsymbol{a}_2 \end{bmatrix} \triangleq \begin{bmatrix} \boldsymbol{r}_1 - \boldsymbol{r}_2 \\ \boldsymbol{a}_1 \ominus \boldsymbol{a}_2 \end{bmatrix} \tag{24a}$$

$$\begin{bmatrix} \boldsymbol{r}_1 \\ \boldsymbol{a}_1 \end{bmatrix} \oplus \begin{bmatrix} \boldsymbol{r}_2 \\ \boldsymbol{r}_3 \end{bmatrix} \triangleq \begin{bmatrix} \boldsymbol{r}_1 + \boldsymbol{r}_2 \\ \boldsymbol{a}_1 \oplus \boldsymbol{r}_3 \end{bmatrix} \tag{24b}$$

$$\begin{bmatrix} \boldsymbol{r}_1 \\ \boldsymbol{a}_1 \end{bmatrix} \otimes \begin{bmatrix} \boldsymbol{r}_2 \\ \boldsymbol{a}_2 \end{bmatrix} \triangleq \begin{bmatrix} \boldsymbol{r}_1 + \mathrm{q2m}(\boldsymbol{a}_1)\boldsymbol{r}_2 \\ \boldsymbol{a}_1 \otimes \boldsymbol{a}_2 \end{bmatrix} \tag{24c}$$

where $\boldsymbol{r}_* \in \mathbb{R}^3$ and $\boldsymbol{a}_* \in \mathbb{H}$. In addition, the time derivative $\circ$ of $\boldsymbol{p} = [\boldsymbol{r}^T, \boldsymbol{a}^T]^T \in \mathbb{P}$ is defined by $\mathring{\boldsymbol{p}} \triangleq [\dot{\boldsymbol{r}}^T, \mathring{\boldsymbol{a}}^T]^T \in \mathbb{R}^6$. Furthermore, the partial derivatives of the addition and multiplication operators can be given as follows:

$$\frac{\mathring{\partial}}{\mathring{\partial}[\boldsymbol{r}_1^T, \boldsymbol{a}_1^T]^T} \begin{bmatrix} \boldsymbol{r}_1 \\ \boldsymbol{a}_1 \end{bmatrix} \oplus \begin{bmatrix} \boldsymbol{r}_2 \\ \boldsymbol{r}_3 \end{bmatrix} \triangleq \begin{bmatrix} \boldsymbol{I} & \boldsymbol{0} \\ \boldsymbol{0} & \mathrm{Exp}(\boldsymbol{r}_3) \end{bmatrix} \tag{25a}$$

$$\frac{\mathring{\partial}}{\partial[\boldsymbol{r}_2^T, \boldsymbol{r}_3^T]^T} \begin{bmatrix} \boldsymbol{r}_1 \\ \boldsymbol{a}_1 \end{bmatrix} \oplus \begin{bmatrix} \boldsymbol{r}_2 \\ \boldsymbol{r}_3 \end{bmatrix} \triangleq \begin{bmatrix} \boldsymbol{I} & \boldsymbol{0} \\ \boldsymbol{0} & \mathrm{Expc}(\boldsymbol{r}_3) \end{bmatrix} \tag{25b}$$

$$\frac{\mathring{\partial}}{\mathring{\partial}[\boldsymbol{r}_1^T, \boldsymbol{a}_1^T]^T} \begin{bmatrix} \boldsymbol{r}_1 \\ \boldsymbol{a}_1 \end{bmatrix} \otimes \begin{bmatrix} \boldsymbol{r}_2 \\ \boldsymbol{a}_2 \end{bmatrix} \triangleq \begin{bmatrix} \boldsymbol{I} & -[(\mathrm{q2m}(\boldsymbol{a}_1)\boldsymbol{r}_2)\times] \\ \boldsymbol{0} & \boldsymbol{I} \end{bmatrix} \tag{25c}$$

$$\frac{\mathring{\partial}}{\mathring{\partial}[\boldsymbol{r}_2^T, \boldsymbol{a}_2^T]^T} \begin{bmatrix} \boldsymbol{r}_1 \\ \boldsymbol{a}_1 \end{bmatrix} \otimes \begin{bmatrix} \boldsymbol{r}_2 \\ \boldsymbol{a}_2 \end{bmatrix} \triangleq \begin{bmatrix} \mathrm{q2m}(\boldsymbol{a}_1) & \boldsymbol{0} \\ \boldsymbol{0} & \mathrm{q2m}(\boldsymbol{a}_1) \end{bmatrix} \tag{25d}$$

where $[\boldsymbol{r}\times]$ is a cross-product matrix, and it is defined as follows:

$$[\boldsymbol{r}\times] \triangleq \begin{bmatrix} 0 & -r_z & r_y \\ r_z & 0 & -r_x \\ -r_y & r_x & 0 \end{bmatrix} \tag{26}$$

Here the functions Exp and Expc are those defined as follows:

$$\mathrm{Exp}(\boldsymbol{r}) \triangleq \sum_{n=0}^{\infty} \frac{[\boldsymbol{r}\times]^n}{n!} \tag{27a}$$

$$\mathrm{Expc}(\boldsymbol{r}) \triangleq \sum_{n=0}^{\infty} \frac{[\boldsymbol{r}\times]^n}{(n+1)!} \tag{27b}$$

From Rodrigues' rotation formula, $\mathrm{Exp}(\boldsymbol{r})$ and $\mathrm{Expc}(\boldsymbol{r})$ can be computed as follows:

$$\mathrm{Exp}(\boldsymbol{r}) = \boldsymbol{I} + [\boldsymbol{r}\times]\,\mathrm{sinc}(\|\boldsymbol{r}\|) + [\boldsymbol{r}\times]^2\,\mathrm{cosc}(\|\boldsymbol{r}\|) \tag{28a}$$

$$\mathrm{Expc}(\boldsymbol{r}) = \boldsymbol{I} + [\boldsymbol{r}\times]\,\mathrm{cosc}(\|\boldsymbol{r}\|) + [\boldsymbol{r}\times]^2\,\mathrm{sincc}(\|\boldsymbol{r}\|) \tag{28b}$$

where $\mathrm{sinc}(x) \triangleq \sin(x)/x$, $\mathrm{cosc}(x) \triangleq (1-\cos(x))/x^2$, and $\mathrm{sincc}(x) \triangleq (x-\sin(x))/x^2$. To avoid the singularity around $x = 0$, these functions should be implemented as follows:

$$\mathrm{sinc}(x) = \begin{cases} \dfrac{\sin(x)}{x} & \text{if } |x| > \varepsilon \\ 1 - \dfrac{x^2}{6}\left(1 - \dfrac{x^2}{20}\left(1 - \dfrac{x^2}{42}\right)\right) & \text{otherwise} \end{cases} \tag{29a}$$

$$\mathrm{cosc}(x) = \begin{cases} \dfrac{1-\cos(x)}{x^2} & \text{if } |x| > \varepsilon \\ \dfrac{1}{2}\left(1 - \dfrac{x^2}{12}\left(1 - \dfrac{x^2}{30}\left(1 - \dfrac{x^2}{56}\right)\right)\right) & \text{otherwise} \end{cases} \tag{29b}$$

$$\mathrm{sincc}(x) = \begin{cases} \dfrac{x-\sin(x)}{x^3} & \text{if } |x| > \varepsilon \\ \dfrac{1}{6}\left(1 - \dfrac{x^2}{20}\left(1 - \dfrac{x^2}{42}\left(1 - \dfrac{x^2}{72}\right)\right)\right) & \text{otherwise} \end{cases} \tag{29c}$$

where ε is a small value and within the ε-neighborhood of $x = 0$, they are replaced by their Maclaurin series. The expressions (28) can be derived through the following property of the cross-product matrix $[\boldsymbol{r}\times]$.

$$[\boldsymbol{r}\times]^3 = -\|\boldsymbol{r}\|^2[\boldsymbol{r}\times] \tag{30}$$

ACKNOWLEDGEMENT

This work was supported by Kobelco Construction Machinery Co., Ltd.

REFERENCES

[1] T. Thalmann, and H. Neuner, "Sensor fusion of robotic total station and inertial navigation system for 6dof tracking applications," *Applied Geomatics*, vol. 16, no. 4, pp. 933–949, 2024.

[2] N. Filipe, M. Kontitsis, and P. Tsiotras, "Extended kalman filter for spacecraft pose estimation using dual quaternions," *Journal of Guidance, Control, and Dynamics*, vol. 38, no. 9, pp. 1625–1641, 2015.

[3] B. Olofsson, J. Antonsson, H. G. Kortier, B. Bernhardsson, A. Robertsson and R. Johansson, "Sensor fusion for robotic workspace state estimation," in *IEEE/ASME Transactions on Mechatronics*, vol. 21, no. 5, pp. 2236–2248, Oct. 2016.

[4] Y. Yamamoto, J. Qiu, T. Doi, T. Nanjo, and K. Yamashita, and R. Kikuuwe, "A position controller for hydraulic excavators with deadtime and regenerative pipelines," *IEEE Transactions on Automation Science and Engineering*, vol. 22, pp. 855–871, 2025.

[5] K. Murata, R. Kikuuwe, T. Okada, H. Yoshihara, T. Doi, T. Nanjo, and K. Yamashita,"Realtime simulation techniques for hydraulic excavators,"in *Proceedings of the 20th SICE System Integration Division Annual Conference*, 2019, pp. 2526–2531, (in Japanese).

[6] R. Kikuuwe, T. Okada, H. Yoshihara, T. Doi, T. Nanjo, and K. Yamashita, "A nonsmooth quasi-static modeling approach for hydraulic actuators," *ASME Journal of Dynamic Systems, Measurement, and Control*, vol. 143, no. 12, p. 121002, 2021.

[7] Y. Yamamoto and R. Kikuuwe, "End-effector position estimation and control of hydraulic excavators with total stations," in *Proceedings of 2024 IEEE/SICE International Symposium on System Integration (SII)*, 2024, pp. 345–350.